



UNICA

UNIVERSITÀ
DEGLI STUDI
DI CAGLIARI



Università di Cagliari

UNICA IRIS Institutional Research Information System

This is the Author's accepted manuscript version of the following contribution:

Di Bernardino, A., Monti, P., Leuzzi, G., & Querzoli, G. (2022). On the Lagrangian and Eulerian time scales of turbulence within a two-dimensional array of obstacles. *Boundary-Layer Meteorology*, 184(2), 375–379. <https://doi.org/10.1007/s10546-022-00717-6>

When citing, please refer to the published version.

This version of the article has been accepted for publication, after peer review (when applicable) and is subject to Springer Nature's AM terms of use, but is not the Version of Record and does not reflect post-acceptance improvements, or any corrections. The Version of Record is available online at: <https://doi.org/10.1007/s10546-022-00717-6>

This full text was downloaded from UNICA IRIS <https://iris.unica.it/>

1 On the Lagrangian and Eulerian Time Scale of the Turbulence 2 within a Two-Dimensional Array of Obstacles

3 Annalisa Di Bernardino¹ • Paolo Monti² • Giovanni Leuzzi² • Giorgio Querzoli³

4 Received: DD Month YEAR/ Accepted: DD Month YEAR/ Published online: DD Month YEAR
5 © Springer Science + Business Media B. V.

6 Abstract

7 Fields of Lagrangian (T^L) and Eulerian (T^E) time scales of the turbulence within a regular
8 array of two-dimensional obstacles of unit aspect ratio have been determined by means of
9 a water-channel experiment reproducing a neutral boundary layer. It has been found a
10 strong spatial inhomogeneity of both the scales and their ratio, $\beta = T^L/T^E$. The results
11 provide useful information for numerical modelling of pollutant dispersion in urban areas.

12 **Keywords** Feature tracking • Canyon • RANS • Turbulence closure • Turbulent dispersion

13 1 Introduction

14 Pollutant dispersion can be simulated numerically via the Lagrangian approach, where the
15 concentration field is calculated by simulating the trajectories of fictitious particles released
16 from the source (Thomson 1987). That requires knowledge of the Lagrangian integral time
17 scale of the turbulence, $T^L = \int_0^\infty \rho^L(\tau) d\tau$ (ρ^L is the Lagrangian autocorrelation function
18 of the velocity (Monin and Yaglom 1971) and $d\tau$ is the time lag). Since the direct
19 measurement of T^L requires particle trajectories long enough to get meaningful ρ^L , its
20 estimation is not an easy task, especially in the case of canopy flows (Shnapp et al. 2020).

21 Knowledge of T^L is also of interest also for simulating pollutant dispersion via the
22 Eulerian approach, in which the concentration can be calculated through Reynolds-
23 averaged Navier–Stokes (RANS) models. As a matter of fact, in this approach, one of the
24 open problems is the choice of the turbulent diffusivity of mass, D_t . Kikumoto (2020)

✉ Paolo Monti
paolo.monti@uniroma1.it

¹ Dipartimento di Fisica, Università di Roma “La Sapienza”, Piazzale Aldo Moro 2, 00185 Rome, Italy

² DICEA, Università di Roma “La Sapienza”, Via Eudossiana 18, 00184 Roma, Italy

³ DICAAR, Università degli Studi di Cagliari, Via Marengo 2, 09123 Cagliari, Italy

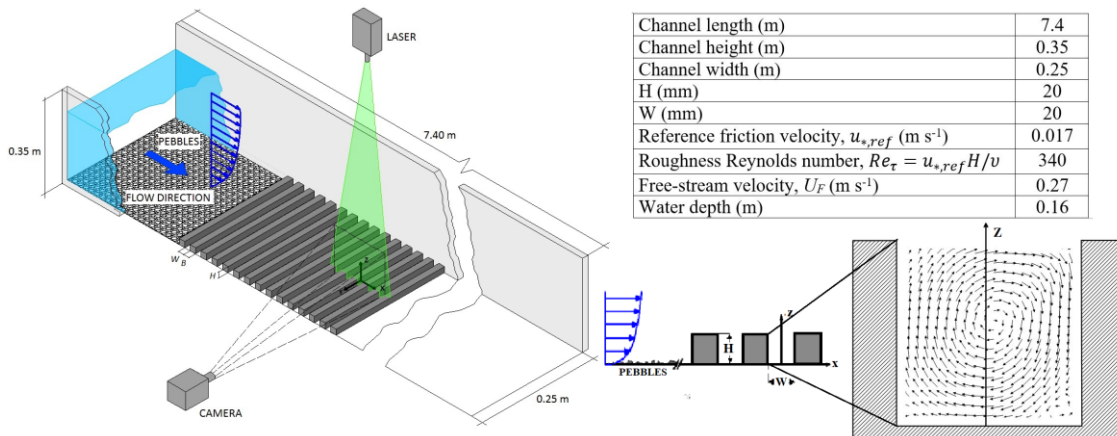
25 introduced the concept of "concentration diffusivity limiter with travel time", by which it
 26 is possible to model D_t with the flight time scaled by T^L .

27 Since Eulerian statistics can be easily determined from fixed-point measurements, a
 28 convenient alternative to the direct estimation of T^L is to measure T^E and then evaluate the
 29 Lagrangian scale by means of the coefficient β : $T^L = \beta T^E$ (Corrsin 1963), where $T^E =$
 30 $\int_0^\infty \rho^E d\tau$ is the Eulerian time scale of the turbulence and ρ^E is the Eulerian velocity
 31 autocorrelation function. β is a parameter greater than unity, whose value is generally
 32 obtained empirically from experimental and numerical experiments (Fattal 2021),
 33 obtaining expressions that are valid for flat terrain (Anfossi et al. 2006), sparse urban
 34 canopies (Nironi et al. 2015), or above arrays of obstacles (Di Bernardino et al. 2017).
 35 However, to our knowledge, β has not still determined within urban canyons.

36 The aim of this study is the evaluation of β within a two-dimensional canyon with unit
 37 aspect ratio (AR=1) that, to our knowledge, has never been investigated.

38 2 Experimental Setup and Time Scales Measurements

39 The experimental set-up and conditions are the same as in Di Bernardino et al. (2015), to
 40 which the reader is referred for all the details. Figure 1 shows the water channel and some
 41 of the main parameters of the experiment. Fluid particle velocities were measured by a
 42 feature tracking technique (Cenedese et al. 2005) over a rectangular region 60 mm long (x-
 43 axis) and 40 mm high (z-axis), lying on the vertical x-z plane passing through the centre
 44 of the channel and aligned with the mean flow.



45
 46 **Fig. 1** Layout of the experimental set-up and list of the main experimental variables. The vector map reports
 47 the average velocity field

48 A 2-mm thick laser light sheet (5-W) illuminated the measurement plane. The framed
49 area was located 30 buildings downstream of the first building so as to minimize any
50 influence from the change in roughness between the roughness elements (pebbles) and the
51 building array. 10,000 images were acquired during the experiment by means of a high-
52 speed video camera at 250 Hz. The dataset consists of about 3000 sparse velocity samples
53 per frame.

54 Both the Eulerian and Lagrangian autocorrelations were calculated in the cavity based
55 on the magnitude of the velocity vector, $u = |\mathbf{u}|$: $\rho^E(\tau) = \overline{(u'(t)u'(t + \tau))} / \sigma^2$, where
56 prime indicates the fluctuation around the mean, the overbar is the time average, σ^2 is the
57 variance of u , and t the time. The trajectories of synthetic fluid particles were reconstructed
58 by integrating the instantaneous (Eulerian) 2D velocity fields following the procedure
59 described in Stocchino et al. (2011). The procedure assumes that crossflow motions are
60 non-dominant as observed in the symmetry plane of two-dimensional canopies by Di
61 Bernardino et al. (2017). Then, $\rho^L(\mathbf{x}, \tau)$, was computed using the expression of the
62 Lagrangian autocorrelation function reported in Di Bernardino et al. (2017) where the
63 details of the procedure can be found. Under the assumption of (Eulerian) statistical
64 stationarity, the statistical ensemble of trajectories used for the computation of the
65 Lagrangian autocorrelation was obtained releasing a set of 50 particles with a random
66 initial position in the neighbourhood of \mathbf{x} (Gaussian distribution with a $0.05H$ standard
67 deviation, with H indicating the building height) at 5 frame intervals, thus resulting in a
68 dataset of 100,000 trajectories per each initial position. Correlations and integral time
69 scales were computed within the canyon on a set of initial positions consisting of a 7×7
70 equispaced grid.

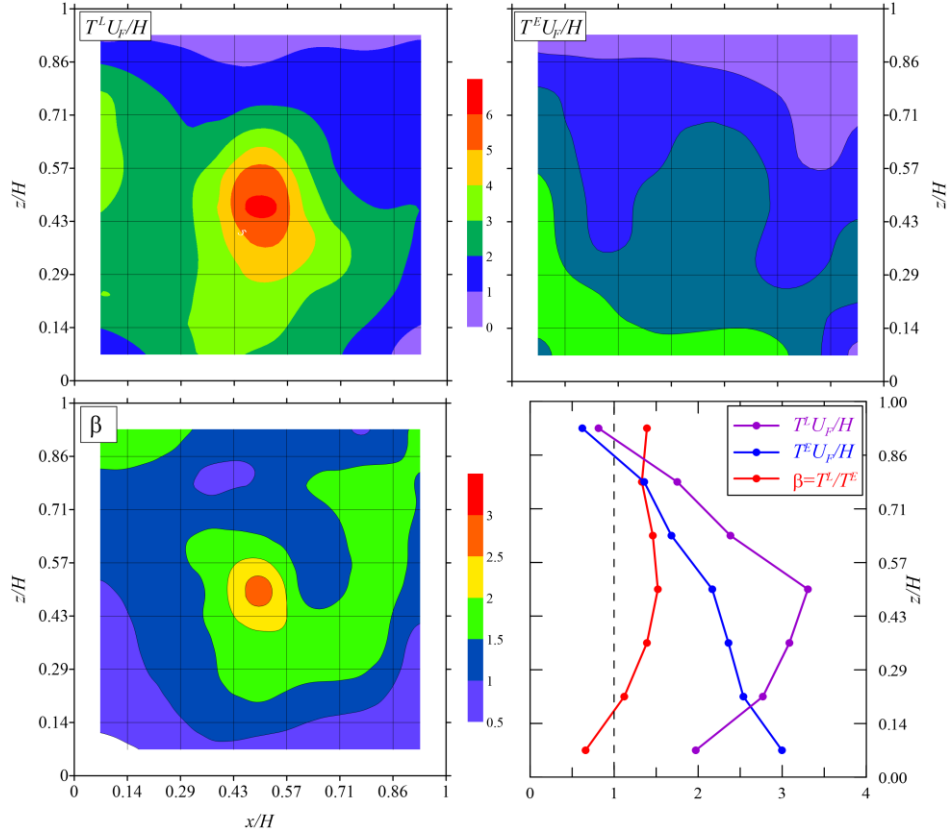
71

72 **3 Results and Discussion**

73 Figure 2a-c show the maps of T^L , T^E , and β , respectively. The reader can refer to Di
74 Bernardino et al. (2015) and (2017) for other turbulence statistics, as well as for the vertical
75 profiles of T^L and T^E above the canopy. Both scales have been normalized by H/U_F ,
76 where U_F is the free-stream velocity. The salient feature of T^L (Fig. 2a) is the presence of
77 a maximum localized at the center of the cavity vortex (see Fig. 1), where particles tend to

78 circulate longer. Lower T^L are confined within the shear layer at the cavity top, which plays
 79 a key role in the exchange of air and scalars between the canopy and the overlying region
 80 (Louka et al. 2000).

81



82

83 **Fig. 2** Maps of T^L (panel a) and T^E (panel b), normalized by T_S and $\beta = T^L/T^E$ (panel c). Panel (d) shows
 84 the vertical profiles of T^L , T^E and β averaged horizontally within the cavity

85

86 It is worth mentioning that the T^L maximum is $\sim 0.5 T_S$ (here, $T_S = H/u_{*,ref} = 1.17 s$
 87 is the characteristic time scale of the cavity), while the mean T^L in the cavity is $\sim 0.15 T_S$.
 88 From this it can be deduced that the assumption of T^L constancy must be taken with the
 89 due caution (see also Fig. 2d, where the vertical profile of T^L averaged along the horizontal
 90 is shown). In contrast, T^E decreases with the height and it is lower than T^L except that near
 91 the bottom. Apart from the lower region, the ratio $\beta = T^L/T^E$ is generally higher than one
 92 and shows a maximum (~ 3) in the middle of the cavity, i.e., where T^L is a maximum.

93

94

The average β in the cavity is about 1.3, not far from $\beta = 1.5$ chosen by Lin et al.
 (2021) in their RANS model to optimize the simulated concentration field within a square

95 cavity ($AR=1$). Conversely, the uneven distribution of T^L differs from that published by
96 Shnapp et al. (2020), where T^L was practically independent of height. A possible reason
97 could be the different geometrical configuration considered by those authors, i.e., a highly
98 inhomogeneous, three-dimensional canopy.

99 **References**

- 100 Anfossi D, Rizza U, Mangia C, Degrazia GA, Pereira Marques Filho E (2006) Estimation of the ratio between
101 the Lagrangian and Eulerian time scales in an atmospheric boundary layer generated by large eddy
102 simulation. *Atmos Environ* 40:326–337
- 103 Cenedese A, Del Prete Z, Miozzi M, Querzoli G (2005) A laboratory investigation of the flow in the left
104 ventricle of a human heart with prosthetic, tilting-disk valves. *Exp Fluids* 39:322–335
- 105 Corrsin S (1963) Estimates of the relations between Eulerian and Lagrangian scales in large Reynolds number
106 turbulence. *J Atmos Sci* 20:115–119
- 107 Di Bernardino A, Monti P, Leuzzi G, Querzoli G (2015) Water-channel study of flow and turbulence past a
108 two-dimensional array of obstacles. *Bound-Layer Meteorol* 155:73–85
- 109 Di Bernardino A, Monti P, Leuzzi G, Querzoli G (2017) Water-channel estimation of Eulerian and
110 Lagrangian time scales of the turbulence in idealized two-dimensional urban canopies. *Bound-Layer*
111 *Meteorol* 165:251–276
- 112 Fattal E, David-Saroussi H, Klausner Z, Buchman O (2021) An Urban Lagrangian Stochastic Dispersion
113 Model for Simulating Traffic Particulate-Matter Concentration Fields. *Atmosphere* 12:580
- 114 Kikumoto H (2020) Turbulent diffusivity limiter with travel time for CFD-Eulerian analysis of point-source
115 pollutant dispersion. *Wind Eng. Res.* 26:148–156.
- 116 Lin C, Ooka R, Kikumoto H, Jia H (2021) Eulerian RANS simulations of near-field pollutant dispersion
117 around buildings using concentration diffusivity limiter with travel time. *Build Environ* 202:108047
- 118 Monin AS, Yaglom AM (1971) *Statistical Fluid Mechanics*. Vol. 1 MIT Press
- 119 Louka P, Belcher SE, Harrison RG (2000) Coupling between air flow in streets and the well-developed
120 boundary layer aloft. *Atmos. Environ.* 34: 2613-2621.
- 121 Nironi C, et al. (2015) Dispersion of a Passive Scalar Fluctuating Plume in a Turbulent Boundary Layer. Part
122 I: Velocity and Concentration Measurements. *Boundary-Layer Meteorol* 156:415–446
- 123 Shnapp R, Bohbot-Raviv Y, Liberzon A, Fattal E (2020) Turbulence-obstacle interactions in the Lagrangian
124 framework: applications for stochastic modeling in canopy flows. *Phys. Rev. Fluids* 5: 094601
- 125 Stocchino A, Besio G, Angiolani S, Brocchini M (2011) Lagrangian mixing in straight compound channels.
126 *J Fluid Mech* 675:168–198
- 127 Thomson DJ (1987) Criteria for the selection of stochastic models of particle trajectories in turbulent flows.
128 *J Fluid Mech* 180:529–556